Src kinases catalytic activity regulates proliferation, migration and invasiveness of MDA-MB-231 breast cancer cells

María Pilar Sánchez-Bailón[a*], Annarica Calcabrini[a,b*], Daniel Gómez-Domínguez[a], Beatriz Morte[c], Esther Martín-Forero[a], Gonzalo Gómez-López[d], Agnese Molinari[b], Kay-Uwe Wagner[e] and Jorge Martín-Pérez[a‡]

[a]Dpto. Biología del Cáncer, Instituto de Investigaciones Biomédicas A. Sols (CSIC/UAM). Arturo Duperier 4, 28029 Madrid, Spain.
[b]Dipartimento Tecnologie e Salute, Istituto Superiore di Sanità, Viale Regina Elena 299, 00161 – Roma, Italy.
[c]Centro de Investigación Biomédica en Red de Enfermedades Raras (CIBERER) Madrid, Spain.
[d]Bioinformatics Unit (UBio), Structural Biology and Biocomputing Programme, Spanish National Cancer Research Centre (CNIO), Madrid.
[e]Eppley Institute for Research in Cancer and Allied Diseases, University of Nebraska Medical Center, 986805 Nebraska Medical Center Rm. 8009, Omaha, NE 68198-6805, USA.

*María Pilar Sánchez-Bailón and Annarica Calcabrini have equally contributed to this work.
‡Corresponding author. Tel.: +34-91-585-4416; Fax: +34-91-585-4401. E-mail address: jmartin@iib.uam.es

Abbreviations used

SFKs, Src family tyrosine kinases; EGF-R, epidermal growth factor receptor; PDGF-R, platelet-derived growth factor receptor; IGF-1R, insulin-like growth factor-1 receptor; VEGF-R, vascular endothelial growth factor receptor; FGF-R, fibroblast growth factor receptor; E-R, Estrogen receptor; PRL-R, Prolactin receptor; DAPI, 4',6-diamidino-2-phenylindole; MTT, 3-(4,5-dimethylthiazol-2-yl)-2,5-diphenyltetra-zolium bromide; BrdU, bromodeoxyuridine; PI, propidium iodide; PARP, poly-ADP ribose polymerase; CSK, C-terminal Src Kinase; GSEA, Gene Set Enrichment Analysis.

Abstract

SFKs are frequently deregulated in cancer where they control cellular proliferation, migration, survival and metastasis. Here we study the role of SFKs catalytic activity in triple-negative/basal-like and metastatic human breast cancer MDA-MB-231 cells employing three well-established inhibitors: Dasatinib, PP2 and SU6656. These compounds inhibited migration and invasion. Concomitantly, they reduced Fak, paxillin, p130CAS, caveolin-1 phosphorylation and altered cytoskeletal structures. They also inhibited cell proliferation, but in different manners. Dasatinib and PP2 increased $p27^{Kip1}$ expression and reduced c-Myc levels, restraining G1-S transition. In contrast, SU6656 did not modify $p27^{Kip1}$ expression, slightly altered c-Myc levels and generated polyploid multinucleated cells, indicating inhibition of cytokinesis. These later effects were also observed in SYF fibroblasts, suggesting a SFKs-independent action. ZM447439, an Aurora B kinase inhibitor, produced similar cell cycle and morphological alterations in MDA-MB-231 cells, indicating that SU6656 blocked Aurora B kinase. This was confirmed by inhibition of histone H3 phosphorylation, the canonical Aurora B kinase substrate. Furthermore, hierarchical clustering analysis of gene expression profiles showed that SU6656 defined a set of genes that differed from Dasatinib and PP2. Additionally, Gene Set Enrichment Analyses revealed that SU6656 significantly reduces the Src pathway. Together, these results show the importance of SFKs catalytic activity for MDA-MB-231 proliferation, migration and invasiveness. They also illustrate that SU6656 acts as dual SFKs and Aurora B kinase inhibitor, suggesting its possible use as a therapeutic agent in breast cancer.

Keywords
SFKs, Dasatinib, PP2, SU6656, Aurora B kinase, MDA-MB-231

1. Introduction

SFKs regulate intracellular signaling pathways originated by activated transmembrane growth factors and cytokines receptors, including EGF-R, PDGF-R, IGF-1R, VEGF-R, FGF-R, HER2, PRL-R, E-R [1-3]. Consequently, SFKs modulate signaling cascades leading to cell proliferation, survival, differentiation, adhesion, migration, invasion, etc., in several biological models [1,4].

Functional deregulation or altered expression of SFKs is associated with human cancers [3,4]. Studies in human samples and animal models support the role of SFKs catalytic activity in tumorigenesis of breast, colorectal, pancreatic, prostatic, melanoma, gastric and ovarian cancers [5]. In breast cancer, increased tyrosine kinase activity of c-Src is associated with induction, progression and metastasis [3,6].

SFKs include nine members (c-Src, Blk, Fyn, Fgr, Hck, Lck, Lyn, Yes and Yrk). They have a modular structure with a membrane-targeting signal, Src homology domains SH2 and SH3 involved in protein-protein interactions. The kinase domain contains the ATP binding site K298 and the autophosphorylation Y418 residue. Phosphorylation of Y530 at carboxyl tail by CSK regulates kinase activity, as it favors intramolecular interactions, which unable SH2, SH3 and catalytic domains functionality [1,4].

SFKs phosphorylate proteins involved in focal adhesion complexes [1,4]. Upon interaction of Src-SH2 domain with auto-phosphorylated Y397-Fak, Src becomes activated and phosphorylates Fak at multiple sites including Y925 [7]. Src-Fak complex controls pathways leading to proliferation, survival, focal adhesion and cytoskeleton remodeling that have also implications in migration and invasiveness [4]. Likewise, Src-Fak complex phosphorylates proteins implicated in focal adhesion, such as paxillin and p130CAS [1,4]. Src also phosphorylates Y14-caveolin-1, which in turns acts as an effector of Rho/ROCK signaling involved in migration and invasion of tumor cells by modulating focal adhesion turnover [8,9]. Furthermore, SFKs catalytic activity is also involved in cell cycle progression. Phosphorylated Y925-Fak by Src serves as docking site for binding of P85-PI3K SH2 domain, leading to stimulation of PI3K/Akt pathway. Also, Src-Fak complex modulates Mek1-2/Erk1-2 pathway [1,2,4].

We previously observed that SFKs catalytic activity regulates the G1-S transition by controlling expression of c-Myc and $p27^{Kip1}$ in MCF7 and T47D non-metastatic human breast cancer cells [2,10] and in lymphoid cells [11,12]. Src phosphorylates $p27^{Kip1}$ on Y74/Y88 facilitating its degradation and, as a result, facilitates G1-S transition [13]. In addition, Src promotes proliferation and survival by activating PI3K/Akt-dependent pathways [12,14].

Together, these data suggest that the SFKs catalytic activity is a potential therapeutic target in several cancers. Thus, targeting the catalytic domain has developed numerous kinase inhibitors, as ATP-competitors. Because structural similarities of ATP pocket among kinases, these compounds are not fully specific for SFKs, instead they are considered as selective inhibitors [15]; such is the case of Dasatinib, PP2 and SU6656. Dasatinib is BCR/Abl and SFKs inhibitor that has additional targets such as c-Kit, Eph kinases [16,17]; it is used in chronic myelogenous leukemia (CML) and is under evaluation for solid tumors including advanced prostate and breast cancer. PP2 shows also weak inhibition to other kinases including EGFR, CK1δ and CSK [18]. SU6656 has some other targets identified in vitro: PDGFR, BRSK2, AMPK, Aurora B kinase, CaMKKβ [18]. The lack of specificity of these inhibitors can be responsible for site-target effects when a single compound is used. To minimize this possible misunderstanding, we carried out studies on the role of SFKs catalytic activity in human

triple-negative/basal like MDA-MB-231 breast cancer cells by employing Dasatinib, PP2 and SU6656.

We show that these three selective inhibitors of SFKs significantly reduced proliferation, migration and invasiveness. Particularly, SU6656 blocked Aurora B kinase and induced polyploidy multinucleated cells blocking cytokinesis. Hierarchical clustering analyses of gene expression profiles show that SU6656 defined an individual set of genes that differed from Dasatinib and PP2. In contrast to them, Gene Set Enrichment Analyses (GSEA) showed that SU6656 significantly reduced Src pathway.

2. Materials and methods

2.1. Reagents

Anti-c-Src 327 was from Calbiochem (Merck4Biosciences, Germany). Anti-Fak (A17), anti-p120-catenin (S-19) and anti-c-Myc (N2E6.2) were from Santa Cruz Biotechnology (Santa Cruz, USA). Anti-pY418-Src, secondary horseradish peroxidase-conjugated antibodies, goat-anti-mouse IgG Alexa-Fluor 488, goat-anti-rabbit IgG Alexa-Fluor 488 or 546 and ProLong antifade-reagent were from Invitrogen (Camarillo, USA). Anti-pY925-Fak, and anti-pY118-paxillin were from Cell Signaling Technologies (Danvers, USA). Anti-paxillin, anti-p130CAS, anti-caveolin, anti-pY14-caveolin, anti-β-catenin, anti-$p27^{Kip1}$, anti-BrdU FITC-conjugated and Matrigel™ were from BD-Biosciences (Bedford, USA). Anti-pS10-histone H3 and anti-phosphotyrosine 4G10 were from Millipore (Billerica, USA). Anti-Aurora B and anti-histone H3 were from ABCAM (Cambridge, UK). Anti-α-tubulin, anti-β-actin, TRITC-labeled phalloidin, DAPI, MTT, BrdU, Trypan blue, propidium iodide (PI) and SU6656 were from Sigma-Aldrich (St. Louis, USA). Purified histone H3 was from Roche Applied Science (Indianapolis, USA). Acrylamide/Bis-acryalamide (29:1), SDS and ammonium persultate were from Bio-Rad Laboratories (Hercules, USA). ECL was from GE Healthcare Biosciences (Pittsburgh, USA). BCA protein assay was from Thermo Scientific (Rockford, USA). PP2 was from Tocris (Ellsville, USA), Dasatinib from LC-Laboratories (Woburn, USA).

2.2. Cell cultures

MDA-MB-231 cells from ATCC were propagated in DMEM supplemented with 5%FCS, 2mM glutamine, 100IU/ml penicillin and 100μg/ml streptomycin.

2.3. Metabolic activity and cell viability studies

For MTT assay, cells were 72h-treated with DMSO (1:1000, Control), Dasatinib (10, 100, 500, 1000nM), PP2 or SU6656 (1, 5, 25, 50μM). Then, 10μl of MTT reagent were added to each well (final concentration 0.5mg/ml) and plates were incubated at 37°C for 4h. After solubilization of formazan crystals (2-3h at 37°C with 10%SDS/10mM HCl), absorbance was measured at 570nm in a VersaMax Elisa Microplate Reader (Molecular Devices, USA). Cell viability was determined by counting cells with Trypan blue. Cells were 72h-treated with DMSO (Control), Dasatinib (100nM), PP2 (5μM) or SU6656 (5μM), then detached, mixed with a 0.4% Trypan blue/PBS solution (1:1), loaded on a hemocytometer and counted.

2.4. Cell cycle analysis

Cell cycle studies were performed by double labeling with BrdU and PI. Cells were pretreated with inhibitors (at concentrations described above) for 2h and pulsed for 30min with BrdU (30μM). Cultures were washed with fresh medium and incubated in the presence or absence of inhibitors for 3, 9, 24 and 36h. Samples were prepared as previously described [10].

For cell cycle studies with PI of 24h- and 72h-treated cells (DMSO, 100nM Dasatinib, 5μM PP2, 5μM SU6656 or 5μM ZM447439), samples were prepared as previously described [10]. Cell acquisition was performed with a FACScan flow

cytometer (BD). At least 10000 events/sample were acquired in linear (for PI) and log (for FITC) mode. The proportion of cells in subG_1, G_1, S, G_2/M, >4N phases was calculated with CellQuest software (BD).

2.5. Cell migration (wound healing assay)

Cells were seeded in complete medium ($8x10^5$ cells/60 mm plate) and grown to confluence. The monolayer was scratched with a 200μl micropipette tip and washed with fresh medium to remove floating cells. Complete medium containing DMSO or inhibitors (concentrations as above) was added to cultures. Photomicrographs were taken at 0h and 20h with a Nikon Eclipse TS100 inverted microscope (Nikon, England), equipped with Olympus DP20 digital camera (Olympus, Germany). Representative fields were photographed. Assays were repeated 3 times. Magnification, X100.

2.6. Invasion assay

Invasiveness was determined using cell culture inserts for 24-well plate (8μm-pore PET membranes) (BD). Filters were coated with 100μl of ice-cold Matrigel diluted in DMEM basal medium and incubated overnight at 37°C. Cells were seeded on the upper chamber ($5x10^4$/well/200μl) in serum-free medium containing DMSO or inhibitors (see migration assay). The lower chamber was filled with 300μl of 10% FBS-supplemented medium and DMSO or inhibitors; 24h later, cells on the top of the inserts were removed and those on the lower surface fixed in methanol, stained with 10µg/ml DAPI/PBS and mounted on slides with ProLong antifade-reagent. Filters were observed with a Plan 20x/0.50 objective using an Axiophot fluorescence microscope (Zeiss, Germany) equipped with an Olympus DP70 digital camera. DAPI-stained nuclei were counted. Assays were performed in triplicate and repeated 4 times.

2.7. Immunofluorescence and confocal microscopy

Cells seeded on sterile coverslips were 24h-treated with DMSO or inhibitors (see above), fixed with 3.7% paraformaldehyde/PBS (10min, room temperature), permeabilized with 0.1% Triton X-100/PBS (5min, room temperature) and blocked 30min with 1% BSA/PBS. Coverslips were incubated 1h at 37°C with 1:200 TRITC-labeled phalloidin (1:200 in PBS-1% BSA) or with anti-α-tubulin (1:50), anti-phospho-histone H3 (1:200), then with goat-anti-mouse IgG Alexa-Fluor 488 or goat-anti-rabbit IgG Alexa-Fluor 546 (1:200) for 1h at 37°C. After washing with PBS, cells were counterstained with 10µg/ml DAPI/PBS for 10min at 37°C and coverslips mounted on slides with ProLong reagent. Samples were observed and photographed with a Plan Apochromat 60x/1.40 objective using a Nikon Eclipse 90i fluorescence microscope equipped with Digital Sight DS-Qi1 camera and Nis-Elements BR imaging software (Nikon).

For confocal microscopy experiments, cells were fixed and permeabilized as above, saturated with 5% goat serum/PBS, washed with PBS-1% BSA. Samples were incubated with anti-pY118-Paxillin (1:50), anti-pY925-Fak (1:50), anti-β-catenin (1:100), anti-p120-catenin (1:100) and with the secondary antibody for 1h at 37°C. Confocal images were acquired using an inverted Zeiss LSM 710 laser-scanning microscope with a Plan Apochromat 60x/1.40 objective. Sequential scanning mode was used to avoid crosstalk between channels. Z-optical stacks with 0.6μm intervals through the cell Z-axis were recorded. Images were processed with ZEN 2009 software (Zeiss)

and Adobe Photoshop CS.

2.8. Time-lapse video microscopy

Live cell imaging was performed with Microscope Cell Observer Z1 system (Carl Zeiss MicroImaging GmbH, Jena, Germany) equipped with a controlled environment chamber (37°C constant temperature, 5% CO_2 atmosphere) and Camera Cascade 1k. MDA-MB-231 cells were seeded in complete medium in 35mm µ-dishes for live cell imaging (10^5 cells/dish) (Ibidi GmbH, Martinsried, Germany). After 24h, cells were treated with DMSO (control) or SU6656 (5µM). Images were collected every 15 min with a 20x Plan Apochromat objective, starting 3h after inhibitor addition until 20h of treatment. Time-lapse movies were formatted using imaging software AxioVision 4.8 (Zeiss) and exported in QuickTime (Apple).

2.9. 3D cell culture assay

Three-dimensional (3D) analysis of morphology was performed as previously described (G.Y. Lee, P.A. Kenny, E.H. Lee, M.J. Bissell, Nature Methods, # 4923). Cell culture dishes (24-well plates) were precoated with 50 µl of undiluted Matrigel (10mg/ml) and incubated for 30min at 37ºC to allow Matrigel to gel. Cells were prepared by trypsinization from tissue culture plastic and resuspension in complete medium (see "Cell cultures" section) for counting. To analyze the effects of SFK selective inhibitors on 3D cell growth, 10^4 cells (per well of a 24-well plate) were resuspended in 300µl of a mixture of complete medium/Matrigel (1:3) containing DMSO (control), Dasatinib (100nM), PP2 (5µM) or SU6656 (5µM). Then, they were seeded over the gelified coat Matrigel and incubated for at least 30min at 37ºC. 500µl of complete medium containing DMSO or SFK selective inhibitors were added to the cultures and changed every 2-3 days until 21 days. To assess the effects of the inhibitors on MDA-MB-231 spheres already formed, drugs were added after a 21-day period of growth and maintained for additional 7 days. Treatments were performed in triplicate and assays were repeated 2 times. Cultures were observed at 10x magnification under a Nikon Eclipse TS100 inverted microscope (Nikon Instruments Europe B.V., Kingston, Surrey, England), equipped with Olympus DP20 digital camera (Olympus Europe GmbH, Hamburg, Germany), and representative fields were photographed.

2.10. Western blotting

Cells were washed in ice-cold PBS, lysed and Western Blot (WB) analyses of phospho-proteins/proteins were carried out as previously described [10].

2.11. Aurora B kinase activity assay

Exponentially growing cultures were lysed at 4°C in lysis buffer (50mM Hepes, pH 8, 600mM KCl, 0.5% Nonidet P40, 1mM Na_3VO_4, 1mM DTT, 0.1mM protease inhibitors). Aurora B kinase was immunoprecipitated from total cell extracts [19]. Immune-complexes were incubated with histone H3 (1µg) for 30min at 37ºC in kinase assay buffer (20mM Hepes, pH 7.4, 150mM KCl, 5mM $MnCl_2$, 5mM NaF, 1mM DTT, 30µM cold ATP) in the presence or absence of 1µM SU6656. pS10-H3, H3 and Aurora B kinase expression was determined by WB.

2.12. Gene expression analyses

Cells cultures (70% confluent) were treated with 100nM Dasatinib, 5μM PP2 or SU6656 for 72h. RNA was isolated using RNeasy kit from Qiagen (Valencia, USA) from three independent experiments carried out in triplicates. After testing for RNA integrity, triplicates RNAs from each treatment/experiment were pooled. Total RNA (10 μg) was used to prepare probes, and then targets were hybridized to "Agilent SurePrint G3 Human GE 8x60k Microarray" (Santa Clara, USA) following manufacture instructions.

Analysis for differential expression was performed using the Rplatform for statistical analysis (R Foundation for Statistical Computing, Vienna) and several packages from the Bioconductor project (http://www.bioconductor.org/). The raw data were imported into R and preprocessed using the half method for background correction and the quantile method for normalization. Probes with expression level below the detection control probe in all samples were removed. To identify differentially expressed genes, we used the limma package. Correction for multiple testing was accomplished by controlling the false discovery rate using the method from Benjamini and Hochberg [20]. Genes were selected as differentially expressed with P*adjust* ≤ 0.05. Hierarchical clustering analysis of gene expression profiles was carried out using the complete linkage method.

2.13. Gene set enrichment analysis (GSEA)

Gene set enrichment analysis [21] was applied using annotations from Biocarta, KEGG and Reactome pathway databases together with Src gene set previously reported [22]. Genes were ranked based on limma moderated t statistic. After Kolmogorov-Smirnoff testing, those gene sets showing FDR ≤ 0.05, were considered significantly enriched amongst compared treatments.

3. Results

3.1. Effect of Dasatinib, PP2 and SU6656 on cell viability, SFKs kinase activity, migration and invasiveness of MDA-MB-231 cells

To determine the concentrations of inhibitors to be used in our study, we tested the effects of 72h-treatment with different concentrations by MTT assay. As observed in Fig. 1A, at 100 nM Dasatinib (Das) and at 5μM PP2 and SU6656 (SU) the mitochondrial metabolic activity was reduced to about 55% respect to control cells (DMSO, vehicle). Viability studies using Trypan blue exclusion test indicated that all three compounds inhibited cell proliferation, as shown by the reduced number of viable cells counted after 72h-treatment (Fig. 1A). Furthermore, the percentage of Trypan blue-positive cells was lower than 5% in all treatments (data not shown), suggesting that, under these experimental conditions, inhibitors were not cytotoxic. Consequently, these concentrations were employed in the following experiments. Furthermore, we determined the effects of inhibitors on three-dimensional growth of MDA-MB-231. When cultures were treated from the beginning, SU6656 inhibited sphere formation (cells were not able to divide and showed enlarged size), while Dasatinib and PP2 reduced sphere size. If inhibitors were added after sphere formation (21 days), control samples showed continuously growing spheres (21+7 days-DMSO), while in the presence of the inhibitors sphere size remained unaltered (21+7 days-PP2 or SU6656) or it clearly appeared reduced (21+7 days-Dasatinib) (Suppl. Figure 1, and Suppl. Materials and methods). DAPI stain of fixed spheres seemed to exclude necrotic/apoptotic cells in treated 3D cultures (data not shown).

Next, we verified if inhibitor concentrations that reduced cell viability and proliferation were able to efficiently inhibit SFKs catalytic activity. To this aim, exponentially growing cultures were treated for 16h with DMSO (vehicle), PP2, SU6656 or Dasatinib. Western blot analyses of lysed cell with anti-phospho-Y418-Src showed that all three compounds clearly reduced phosphorylation of Y418-Src (Fig. 1B).

The oncogenic potential of increased SFKs catalytic activity in tumor cells is pleiotropic and controls cytoskeletal-linked events, such as extracellular matrix-adhesion, migration, and invasion, which are associated to SFKs substrates including Fak, p130CAS and paxillin involved in integrin signaling and in adhesion dynamics [1,4]. We have then analyzed whether SFKs inhibitors affected the phosphorylation of these proteins. Phosphorylation of Y925-Fak by Src observed in DMSO-treated cells was inhibited upon 24h treatment with Dasatinib, PP2 or SU6656 (Fig. 1C).

Activated Src-Fak complex engages and phosphorylates other proteins of focal adhesion complex, including paxillin and p130CAS [10]. Dasatinib, PP2 or SU6656, employed as above, strongly reduced Y118-paxillin phosphorylation as compared to DMSO-treated cells. Likewise, the amount of tyrosine-phosphorylated p130CAS was also diminished (Fig. 1C, IP p130CAS /WB pY).

Caveolin-1, a multifunctional membrane protein responsible for caveolae formation, is phosphorylated by SFKs at Y14 and mediates tumor migration and invasion through Rho/ROCK [9]. As observed here, these inhibitors clearly reduced pY14-caveolin as compared to control cells (Fig. 1C). Furthermore, we tested by confocal microscopy the expression and distribution of pY118-paxillin and pY925-Fak and their relationship with actin cytoskeleton (phalloidin-TRITC labeling). In control cells pY118-paxillin and pY925-Fak accumulated in focal adhesion area; after inhibitor

treatments a consistent reduction of pY118-paxillin and pY925-Fak was observed (Suppl. Fig. 2 and 3). Actin cytoskeleton, characterized by stress fibers in untreated samples, showed a thickness of these structures at the cell edge after PP2 treatment. Dasatinib caused alterations of cytoskeleton structure with collapse of actin microfilaments. SU6656-treated cells maintained actin stress fibers, although in some cells, a thickening of these filaments was observed at the edges (Suppl. Fig. 2 and 3).

Since these inhibitors altered focal adhesion molecules and actin structures, we analyzed subcellular localization of β-catenin and p120 catenin. Treatments increased membrane-localized β-catenin and p120 catenin (Suppl. Fig. 4 and 5), while the total levels of both proteins remained unchanged, as observed by Western Blot (data not shown).

Inhibition of focal adhesion proteins phosphorylation and altered cellular distribution of catenins should lead to a reduction in adhesion dynamics and to inhibition of migration and invasion. To test this hypothesis, we determined the migration and invasion capability of MDA-MB-231 cells upon treatment with SFKs inhibitors. Migration assayed by wound healing repair showed that control cells migrated to heal the wound. Treatments with Dasatinib, PP2 and SU6656 clearly reduced cell migration (Fig. 1D). For invasion assay, cells treated with DMSO, Dasatinib, PP2 or SU6656 were loaded on the top of Matrigel in a Boyden chamber; those able to move throughout this extracellular matrix were then counted as a measurement of invasion (see Materials and methods). All three inhibitors significantly reduced cell invasion (Fig. 1E), suggesting that SFKs catalytic activity is involved in MDA-MB-231 cell migration and invasion processes.

3.2. Effects of SFKs inhibitors on cell cycle progression and morphology of MDA-MB-231 cells and SYF fibroblasts

Inhibition of cell proliferation induced by SFKs inhibitors could be ascribed to alteration of cell cycle progression. Studies performed by double labeling with BrdU and PI showed that treatment with Dasatinib or with PP2 induced G1 accumulation and reduced the number of cells in S or G2/M compartments as compared to control cells (Fig. 2A). Surprisingly, SU6656 caused an aberrant cell cycle; G1 and S phases decreased with time, and the G2/M started to decline after 24h. A new set of cells that accumulated DNA (>4N) increased constantly (Fig. 2A). Thus, Dasatinib and PP2 appeared to affect G1-S transition, while SU6656 generated polyploidy.

To confirm these results, cell cycle was analyzed at longer time (72h) by PI labeling. Dasatinib and PP2 caused accumulation of cells in G1 and reduced the number of cells in S and G2/M phases. The >4N compartment was minimal as in control cells (Fig. 2B). SU6656 reduced cells in G1 and S compartments, increased cells in G2/M and provoked a 60% increase of polyploid cells (Fig. 2B). Consistently, this compound did not inhibit DNA duplication, but it probably blocked completion of cell cycle, which is reliable with the strong reduction of cell number determined by Trypan Blue (Fig. 1A). It should be noticed that, besides the absence of cells in Sub-G1, no PARP degradation was detected (data not shown), suggesting that these compounds, under these experimental conditions, did not induce apoptosis.

In agreement with accumulation of cells in G1 upon treatment with Dasatinib and PP2, $p27^{Kip1}$ expression increased and c-Myc levels decreased as compared to control growing cells (Fig. 2C). Since SU6656 did not alter G1-S transition, expression of $p27^{Kip1}$ and c-Myc were similar to control cultures (Fig. 2C).

The differential effects induced by SU6656 as compared to Dasatinib and PP2 on viability, proliferation and cell cycle progression may be reflected on cell morphology. Then, we carried out double immunofluorescence labeling of nuclei and microtubules (see Materials and methods). Dasatinib-treated cells showed partially collapsed microtubule structure defining a pseudo-spherical shape (Fig. 2D). Tubulin staining pattern induced by PP2 was relatively similar to control cells, although cells adopted an elongated morphology (Fig. 2D). In SU6656-treated cells, microtubule cytoskeleton was also maintained. However, cell size clearly increased and multinucleation was induced (arrows indicated an example of several nuclei within a cell) (Fig. 2D), supporting the hypothesis that SU6656 blocked cell division.

To confirm this blockage, we carried out a 24h video-microscopy of cells treated with DMSO or with SU6656. While control cells divided along the time course of the experiment, SU6656-treated cells detached from the culture plate and before completing cell division re-attached giving rise to bigger multinucleated cells (Suppl. Videos 1,2).

These findings suggest that SU6656, in addition to inhibit SFKs, was affecting other targets that, in turn, could account for this unusual response as compared to Dasatinib and PP2. To support this hypothesis, we investigated whether SU6656 provoked similar cell cycle and morphological alterations in cells that do not express SFKs, such as mouse SYF fibroblast derived from triple deletion of *c-src*, *yes* and *fyn* [23]. Cell cycle analyses after PI labeling showed that 24h treatment with Dasatinib or PP2 had no effects as compared with DMSO-treated cells (Fig. 3A), which is consistent with the fact that SYF fibroblasts do not express SFKs. SU6656 strongly reduced cells in G1 and S phases and increased the number of cells in G2/M and >4N compartments (Fig. 3A). Consistently, Dasatinib or PP2 did not significantly alter cell morphology as compared to control cultures (Fig. 3B). In contrast, SU6656 produced enlarged multinucleated cells (arrows indicated several nuclei within a cell) (Fig. 3B). Together, these results resemble those induced by SU6656 in MDA-MB-231 cells (Fig. 2B and D). It should be noted that SU6656 caused similar alterations in MCF7 and SUM159 human breast cancer cell lines (data not shown), suggesting that SU6656-mediated cell cycle alteration is a common effect in breast cancer cells.

3.3. Differential effects of SU6656 versus Dasatinib and PP2: inhibition of Aurora B kinase

Blockage of cell division by SU6656 suggests that a kinase involved in regulation of mitosis and cell division could also be affected. Among these enzymes, Aurora B kinase, which inhibition causes polyploidy in a variety of human tumor cell lines [24], is inhibited in vitro by SU6656 [18,25]. Therefore, we compared the effects of SU6656 (5μM) and ZM447439 (5μM), a selective inhibitor of Aurora B kinase [19,26], on cell cycle progression and morphology of MDA-MB-231 cells. After 24h treatment, cell cycle analyses by PI labeling showed that both inhibitors reduced cells in G1 and S phases and robustly increased cells in G2/M and > 4N compartments (Fig. 4A). Immunofluorescence analyses showed that both SU6656 and ZM447439 induced multinucleated cells (arrows indicated several nuclei within a cell) (Fig. 4B). Since serine-10 of histone H3 is a canonical substrate for Aurora B kinase [19,24,26,27], we investigated whether SU6656 blocked this phosphorylation, using ZM443979-treated cells as a positive control. Exponentially growing cultures treated 24h with SU6656 or with ZM443979 showed strong reduction of pS10-H3 as compared to control cultures (Fig. 4C). We then immunoprecipitated Aurora B kinase from cultures treated for 24 h with DMSO or with SU6656 and carried out in vitro kinase assay using purified histone

H3 as a substrate (see Materials and methods). The level of pS10-H3 detected in immuno-complexes from SU6656 treated cells was strongly diminished as compared to those from control cells (Fig. 4D). As the amounts of H3 and Aurora B kinase in the immuno-complex reactions were similar, it can be argued that SU6656 inhibited Aurora B kinase activity in MDA-MB-231 cells. Fluorescence microscopy of mitotic cells stained with DAPI, α-tubulin and pS10-H3 confirmed these results. As compared to control cells, 24 h treatment with SU6656 or with ZM443979 induced the appearance of cells with multiple spindle poles and drastic reduction of pS10-H3 staining (Fig. 4E), a characteristic phenotype of Aurora B kinase-inhibited cells [28]. Together these data showed that SU6656 mimicked the effects of ZM443979 in cell cycle, morphology and histone H3 phosphorylation and suggest that SU6656 inhibited cell division of MDA-MB-231 cells by blocking the functionality of Aurora B kinase.

3.4. Differential gene expression induced by Dasatinib, PP2 and SU6656

In view of the differential responses of SU6656 versus Dasatinib and PP2 for cell cycle regulation, we engaged analyses of gene expression profiles induced by these compounds. All studies were carried out in triplicates and RNA was used to hybridize Agilent microarrays. One of SU6656 triplicates was discarded because it did not pass quality control standards. All treatments resulted in gene expression changes. Using a statistical cut-off of P*adjust*≤0.05, we obtained 1866 differentially expressed probes (1641 annotated sequences) after Dasatinib treatment, 21 after SU6656 (15 annotated sequences) and 16 probes after PP2 treatment. The complete list of genes is provided in Suppl. Table I. The hierarchical clustering of all individual data representing all selected differentially expressed sequences is shown in Fig. 5A. The columns contain data for individual samples, which clustered in four groups as a function of treatment, and indicated that replicates were fairly homogeneous. The rows show relative intensities of the probes and defined two main clusters of differentially expressed genes, having higher or lower expression after treatments. The results revealed that the effects of Dasatinib were more pronounced than those of PP2, although in most cases there was also an effect, but of lower intensity. This gene expression pattern did not correspond to that observed for SU6656 treatment, which is more similar to DMSO-treated cells (Control). The comparisons of each individual treatment versus control using plot profile representations is shown in Fig. 5B. These plots show expression values along different samples for probes selected as differentially expressed in the three treatment groups. The data indicated again that Dasatinib produced large changes of gene expression that diverged to control and SU6656 samples and to lower degree to PP2. Although only a reduced number of genes passed the statistical analysis after PP2 treatment, the plots showed that there was a great agreement between PP2 and Dasatinib. The PP2 versus Control analysis showed two main clusters, PP2-Dasatinib, and SU6656-Control. Instead, in the evaluation of SU6656 versus Control, a set of genes defined in an individual group that differed from the rest of treatments. In addition, almost all genes selected in PP2 and Dasatinib groups did not alter their expression after SU6656 treatment.

Furthermore, to study pathways of gene expression related to biological functions analyzed above upon different treatments, GSEA [21] was applied using annotations from Biocarta, KEGG and Reactome pathway databases together with Src gene set previously reported [22]. The analyses (Suppl. Table II) showed that most of the pathways detected were down regulated in each treatment. Exceptionally, glycolysis was upregulated in Dasatinib-treated cells, while asthma and autoimmune thyroid

disease were increased in PP2-treated cells. Some pathways were shared by Dasatinib, PP2 and SU6656, while others appears to be more specific. These pathways can be summarized in main categories. Common to all three treatments are pathways involved in different processes of cell cycle regulation, immune system and metabolism of lipids and lipoproteins. Dasatinib and PP2 shared pathways involved in signaling by EGFR in cancer, by GPCR and by NGF. In addition of cell cycle regulation, metabolism of carbohydrates was common in PP2 and SU6656, while pathways involved in renal cell carcinoma, pancreatic, bladder and colorectal cancer and WNT signaling appeared to be specific for SU6656. Interestingly, GSEA analyses of Src gene pathway (Suppl. Table III) showed a significant reduction upon SU6656 treatment (FDR =0.024), while PP2 and Dasatinib treatments had FDR >0.05 (0.083 and 0.193, respectively).

4. Discussion

SFKs regulate signaling pathways engaged in the control of many cellular processes. As they are frequently deregulated in numerous tumors including breast cancer [3-6], their catalytic activity has been considered as a target for cancer therapy. Since there are not fully specific inhibitors of SFKs, here, we studied the role of SFKs catalytic activity in human triple-negative/basal-like MDA-MB-231 breast cancer cells employing Dasatinib, PP2 and SU6656 selective inhibitors. Interestingly, while these compounds inhibited pY418-Src, GSEA analysis showed that Src gene set expression was significantly reduced by SU6656. All three compounds significantly reduced cellular proliferation, migration and invasion.

SFKs, directly or through a complex with Fak, control pathways involved in the dynamics of focal adhesions, which are engaged in the regulation of cellular migration and invasiveness [1,4]. Thus, Src/Fak phosphorylates proteins of the focal adhesion complex including paxillin, p130CAS, as well as caveolin-1. Consistent with inhibition of SFKs catalytic activity by Dasatinib, PP2 and SU6656, tyrosine phosphorylation of paxillin, p130CAS and caveolin-1 was reduced, cytoskeleton architecture was altered and cellular migration and invasiveness were also inhibited. In this context, we previously showed that the functionality of SFKs was essential for cellular migration, spreading and adhesion of MCF7 cells [10]. Here, we observed that migration of SYF fibroblasts, which lack SFKs, was not altered by Dasatinib, PP2 or SU6656 treatments (data not shown). Together, these data suggest that reduction caused in MDA-MB-231 cells by these compounds could be ascribed to inhibition of SFKs catalytic activity.

Concomitantly, GSEA analysis of the gene expression patterns showed that these inhibitors also down-regulated several pathways associated with migration, cell motility and cytoskeleton reorganization, which in turn could affect cell invasion.

Studies in different tumor cells support these results. Dasatinib reduced migration and invasion in head and neck squamous cell carcinoma, non–small cell lung cancer [29] and in breast cancer cell lines [30,31]. Interestingly, basal-like/triple-negative breast cancer cell lines with high levels of caveolin-1 expression, like MDA-MB-231 cells, are characterized by sensitivity to Dasatinib, while low expression of caveolin-1 correlates with resistance [32]. In MDA-MB-231 and BT-549, inhibition of SFKs by SU6656 suppresses invadopodia formation while enhances tubulin-based microtentacle, effects associated with reduced cellular invasion [33]. PP2 also inhibits invasion in MDA-MB-231 [34] and ovarian cancer cells [35].

Dasatinib, PP2 and SU6656 significantly reduced cell proliferation and specifically altered cellular morphology. Dasatinib generated pseudo-spherical cells, PP2 caused elongated spindle morphology and SU6656 produced flattened enlarged cells, indicating that they affected additional targets. SU6656 similarly altered morphology of SYF fibroblasts, while Dasatinib and PP2 did not. Therefore, the changes induced by SU6656 in MDA-MB-231 seem to be independent on SFKs catalytic activity. Our results concerning effects of Dasatinib on cell proliferation are similar to those previously described [30]. Others have reported that Dasatinib induces cell death and apoptosis in tumor cell lines including MDA-MB-468 [36], head and neck squamous cell carcinoma, non-small cell lung cancer cells and in osteosarcoma and Ewing's subset of bone sarcomas [29,37]. In contrast, in our study Dasatinib, PP2 and SU6656 did not induce cytotoxic effects.

Concomitant with inhibition of cell proliferation, Dasatinib and PP2 reduced c-Myc expression and increased $p27^{Kip1}$ levels, which are consistent with a blockage of cell cycle progression in G1. Dasatinib and PP2 produced similar results in studies

conducted in MDA-MB-231, W53 lymphoid cells, MCF7 and in ovarian cancer cells [2,11,30,35]. Also, interfering SFKs functionality by conditional expression of SrcDN in MCF7 cells causes accumulation in G1 and increased $p27^{Kip1}$ expression [10].

Interestingly, SU6656 neither blocked G1 to S transition, nor induced $p27^{Kip1}$ expression, causing only a small reduction of c-Myc levels. Instead, SU6656 caused polyploidy. These findings could explain the quantitative differences observed between Trypan blue and MTT proliferation assays. In Trypan blue assays, SU6656 induced an inhibitory effect more evident (80%) than Dasatinib or PP2 (25-35%), while in MTT assays the inhibition was quite similar (approximately 45%). Analyzing cell cycle progression with BrdU/PI labeling at 24h or with PI at 72h solved discrepancy between these two methods. In both assays, Dasatinib and PP2 increased cell number in G1, suggesting that they blocked G1-S transition. Consistently, GSEA analysis showed that G1/S transition pathway (Reactome) is down regulated in Dasatinib and PP2-treated cells (FDR $\leq 1x10^{-6}$). In contrast, SU6656 caused accumulation of large polyploid multinucleated cells, suggesting that it did not block cell cycle at a particular phase. Instead, cells seemed to enter and go out of mitosis but failed to divide. This implies that cell continued to be metabolically active in order to synthesize all components necessary for cycling, which explains higher values obtained with MTT than with Trypan blue assay. Indeed, time-lapse video microscopy showed that SU6656 treated cells detached from the substrate just before cell division but, in contrast to dividing control cells, they re-attached and did not complete cytokinesis, generating enlarged cells. SU6656 also induced polyploidia and multinucleation of SUM159 and MCF7 human breast cancer cell lines (data not shown). Since MCF7 has a functional p53, while MDA-MB-231 and SUM159 have p53 mutated [38], these effects appear to be p53 independent.

Polyploidy has been also observed in B-lymphocytes, non-Hodgkin's lymphoma and megakaryocytic cells upon treatment with SU6656 [25,39]. SU6656 caused similar effects in SYF, indicating that SU6656 is targeting additional kinases involved in cell division. Indeed, SU6656 inhibits Aurora B kinase in vitro [18]. It is well established that Aurora B kinase, in addition to phosphorylate S10-H3, is a spindle checkpoint kinase required for cytokinesis and its inhibition eliminates mitotic checkpoint generating polyploid multinucleated cells [24]. We found that ZM447439, a known inhibitor of Aurora B kinase [19,26], produced similar effects as SU6656 in cell cycle progression, morphological alterations and inhibition of S10-H3 phosphorylation in MDA-MB-231 cells. Furthermore, SU6656 also inhibited Aurora B kinase in these cells. Similar results were observed in megakaryocytic [25] and MCF7 cells [27].

Since Aurora B kinase is required for completion of mitosis, chromosome segregation and cytokinesis, and is up-regulated in a variety of tumors, it is considered as relevant target in cancer therapy [40,41]. In this context, AZD1152, another Aurora B kinase inhibitor, blocks proliferation in human breast cancer cell lines and reduces lung metastasis of MDA-MB-231 in nude mouse [42].

In conclusion, our results in human metastatic breast cancer cells indicate that SFKs catalytic activity is required for proliferation, migration and invasiveness, through the regulation of molecular pathways involved in these cellular processes. Of particular interest is SU6656 that being a dual SFKs/Aurora B kinase inhibitor could have a potential use as a therapeutic agent in metastatic breast cancer.

Acknowledgments

Authors are thankful to J. León, A. Sánchez-Pacheco, A. Muñoz, A. Zambrano, A. Aranda for comments and suggestions and L. Naranjo-Valencia and N. Guillén Díaz-Maroto for assistance. This work was supported by grants from Ministerio de Ciencia e Innovación [SAF2009-09254] and Fundación de Investigación Médica Mutua Madrileña. MP. S-B. was supported by a FPI fellowship from Ministerio de Ciencia e Innovación, and A.C. was partially supported by a grant from Fundación de Investigación Médica Mutua Madrileña. J. MP. Is a member of GEICAM.

Authorship

M.P. Sánchez-Bailón, A. Calcabrini, D. Gómez-Domínguez, E. Martín-Forero and J. Martín-Pérez performed experiments, analyzed the data, made figures and reviewed the manuscript; B. Morte and G. Gómez-López analyzed microarrys data and contributed to write the manuscript; A. Molinari and K-U. Wagner discussed the experimental data and contributed to write the manuscript; J. Martín-Pérez conceived and designed the experiments, analyzed the data, and wrote the manuscript.

References

[1] S.M. Thomas, J.S. Brugge, Ann. Rev. Cell. Dev. Biol. 13 (1997) 513-609.
[2] J.J. Acosta, R.M. Munoz, L. Gonzalez, A. Subtil-Rodriguez, M.A. Dominguez-Caceres, J.M. Garcia-Martinez, A. Calcabrini, I. Lazaro-Trueba, J. Martín-Pérez, Mol. Endocrinol. 17 (2003) 2268-2282.
[3] E.L. Mayer, I.E. Krop, Clin. Cancer Res. 16 (2010) 3526-3532.
[4] M. Guarino, J. Cell. Physiol. 223 (2010) 14-26.
[5] J.M. Summy, G.E. Gallick, Cancer Metastasis Rev. 22 (2003) 337-358.
[6] X.H. Zhang, Q. Wang, W. Gerald, C.A. Hudis, L. Norton, M. Smid, J.A. Foekens, J. Massague, Cancer Cell. 16 (2009) 67-78.
[7] V.G. Brunton, E. Avizienyte, V.J. Fincham, B. Serrels, C.A. Metcalf, 3rd, T.K. Sawyer, M.C. Frame, Cancer Res. 65 (2005) 1335-1342.
[8] T.M. Williams, M.P. Lisanti, Am. J. Physiol. Cell Physiol. 288 (2005) C494-506.
[9] B. Joshi, S.S. Strugnell, J.G. Goetz, L.D. Kojic, M.E. Cox, O.L. Griffith, S.K. Chan, S.J. Jones, S.P. Leung, H. Masoudi, S. Leung, S.M. Wiseman, I.R. Nabi, Cancer Res. 68 (2008) 8210-8220.
[10] L. Gonzalez, M.T. Agullo-Ortuno, J.M. Garcia-Martinez, A. Calcabrini, C. Gamallo, J. Palacios, A. Aranda, J. Martin-Perez, J. Biol. Chem. 281 (2006) 20851-20864.
[11] J.A. Fresno Vara, M.A. Dominguez Caceres, A. Silva, J. Martín-Pérez, Mol. Biol. Cell. 12 (2001) 2171-2183.
[12] M.A. Dominguez-Caceres, J.M. Garcia-Martinez, A. Calcabrini, L. Gonzalez, P.G. Porque, J. Leon, J. Martin-Perez, Oncogene 23 (2004) 7378-7390.
[13] M. Grimmler, Y. Wang, T. Mund, Z. Cilensek, E.M. Keidel, M.B. Waddell, H. Jakel, M. Kullmann, R.W. Kriwacki, L. Hengst, Cell 128 (2007) 269-280.
[14] R.H. Medema, G.J. Kops, J.L. Bos, B.M. Burgering, Nature. 404 (2000) 782-787.
[15] T. Chen, J.A. George, C.C. Taylor, Anticancer Drugs 17 (2006) 123-131.
[16] L.J. Lombardo, F.Y. Lee, P. Chen, D. Norris, J.C. Barrish, K. Behnia, S. Castaneda, L.A. Cornelius, J. Das, A.M. Doweyko, C. Fairchild, J.T. Hunt, I. Inigo, K. Johnston, A. Kamath, D. Kan, H. Klei, P. Marathe, S. Pang, R. Peterson, S. Pitt, G.L. Schieven, R.J. Schmidt, J. Tokarski, M.L. Wen, J. Wityak, R.M. Borzilleri, J. Med. Chem. 47 (2004) 6658-6661.
[17] J. Das, P. Chen, D. Norris, R. Padmanabha, J. Lin, R.V. Moquin, Z. Shen, L.S. Cook, A.M. Doweyko, S. Pitt, S. Pang, D.R. Shen, Q. Fang, H.F. de Fex, K.W. McIntyre, D.J. Shuster, K.M. Gillooly, K. Behnia, G.L. Schieven, J. Wityak, J.C. Barrish, J. Med. Chem. 49 (2006) 6819-6832.
[18] J. Bain, L. Plater, M. Elliott, N. Shpiro, C.J. Hastie, H. McLauchlan, I. Klevernic, J.S. Arthur, D.R. Alessi, P. Cohen, Biochem. J. 408 (2007) 297-315.
[19] M. Tardaguila, E. Gonzalez-Gugel, A. Sanchez-Pacheco, Mol. Endocrinol. 25 (2011) 385-393.
[20] Y. Benjamini, Y. Hochberg, J. R. Stat. Soc. Ser. B 57 (1995) 289-300.
[21] A. Subramanian, P. Tamayo, V.K. Mootha, S. Mukherjee, B.L. Ebert, M.A. Gillette, A. Paulovich, S.L. Pomeroy, T.R. Golub, E.S. Lander, J.P. Mesirov, Proc. Natl. Acad. Sci. U S A 102 (2005) 15545-15550.
[22] A.H. Bild, A. Potti, J.R. Nevins, Nat. Rev. Cancer 6 (2006) 735-741.
[23] R.A. Klinghoffer, C. Sachsenmaier, J.A. Cooper, P. Soriano, EMBO J. 18 (1999) 2459-2471.
[24] R. Giet, C. Petretti, C. Prigent, Trends Cell Biol. 15 (2005) 241-250.

[25] B.J. Lannutti, N. Blake, M.J. Gandhi, J.A. Reems, J.G. Drachman, Blood 105 (2005) 3875-3878.
[26] C. Ditchfield, V.L. Johnson, A. Tighe, R. Ellston, C. Haworth, T. Johnson, A. Mortlock, N. Keen, S.S. Taylor, J. Cell Biol. 161 (2003) 267-280.
[27] J.L. Riffell, R.U. Janicke, M. Roberge, Mol Cancer Ther. 10 (2011) 839-849.
[28] Y. Tao, P. Zhang, F. Girdler, V. Frascogna, M. Castedo, J. Bourhis, G. Kroemer, E. Deutsch, Oncogene 27 (2008) 3244-3255.
[29] F.M. Johnson, B. Saigal, M. Talpaz, N.J. Donato, Clin. Cancer Res. 11 (2005) 6924-6932.
[30] C.S. Pichot, S.M. Hartig, L. Xia, C. Arvanitis, D. Monisvais, F.Y. Lee, J.A. Frost, S.J. Corey, Br. J. Cancer 101 (2009) 38-47.
[31] Y.L. Choi, M. Bocanegra, M.J. Kwon, Y.K. Shin, S.J. Nam, J.H. Yang, J. Kao, A.K. Godwin, J.R. Pollack, Cancer Res. 70 (2010) 2296-2306.
[32] F. Huang, K. Reeves, X. Han, C. Fairchild, S. Platero, T.W. Wong, F. Lee, P. Shaw, E. Clark, Cancer Res. 67 (2007) 2226-2238.
[33] E.M. Balzer, R.A. Whipple, K. Thompson, A.E. Boggs, J. Slovic, E.H. Cho, M.A. Matrone, T. Yoneda, S.C. Mueller, S.S. Martin, Oncogene 29 (2010) 6402-6408.
[34] S. Mehrotra, L.R. Languino, C.M. Raskett, A.M. Mercurio, T. Dohi, D.C. Altieri, Cancer Cell 17 (2010) 53-64.
[35] M. Aponte, W. Jiang, M. Lakkis, M.J. Li, D. Edwards, L. Albitar, A. Vitonis, S.C. Mok, D.W. Cramer, B. Ye, Cancer Res. 68 (2008) 5839-5848.
[36] J. Nautiyal, P. Majumder, B.B. Patel, F.Y. Lee, A.P. Majumdar, Cancer Lett. 283 (2009) 143-151.
[37] A.C. Shor, E.A. Keschman, F.Y. Lee, C. Muro-Cacho, G.D. Letson, J.C. Trent, W.J. Pledger, R. Jove, Cancer Res. 67 (2007) 2800-2808.
[38] M. Wasielewski, F. Elstrodt, J.G. Klijn, E.M. Berns, M. Schutte, Breast Cancer Res. Treat. 99 (2006) 97-101.
[39] N. Dussault, C. Simard, S. Neron, S. Cote, Blood Cells Mol. Dis. 39 (2007) 130-134.
[40] M.A. Hardwicke, C.A. Oleykowski, R. Plant, J. Wang, Q. Liao, K. Moss, K. Newlander, J.L. Adams, D. Dhanak, J. Yang, Z. Lai, D. Sutton, D. Patrick, Mol. Cancer Ther. 8 (2009) 1808-1817.
[41] N. Keen, S. Taylor, Cancer Metastasis Rev. 28 (2009) 185-195.
[42] C.P. Gully, F. Zhang, J. Chen, J.A. Yeung, G. Velazquez-Torres, E. Wang, S.C. Yeung, M.H. Lee, Mol. Cancer 9 (2010) 42.

Figure legends

Fig. 1. Effect of Dasatinib, PP2 and SU6656 on MDA-MB-231 viability, SFKs catalytic activity, migration and invasion. A) Cells seeded in 96-well plates ($1.8x10^4$ cells/well) were incubated for 72h with Dasatinib (Das), PP2 or SU6656 (SU). Metabolic activity (%) was calculated considering the value of control (DMSO-treated) at 72h as 100%. For Trypan blue assay, cells plated in 35 mm-dishes were treated with DMSO (C, control), Das (100nM), PP2 (5μM) or SU (5μM) for 72h and then counted in the hemocytometer with 0.4% Trypan blue solution. Percentage of viable cells was calculated considering the value from control sample as 100%. Results represent the average and standard deviations (SD, bars) of three independent experiments carried out in triplicate; asterisks indicate significant differences between treated and control cells (*** $p \leq 0.001$). B) Extracts from cells incubated with DMSO (1:1000), PP2 (5μM), SU (5μM) or Das (100nM) for 16h were blotted with anti-pY418-Src, anti-c-Src (327) and anti-β-actin for loading control. Results are representative of three independent experiments. Ratios of pY418-Src/Src and pY418-Src/β-actin were determined by densitometry and values normalized versus control cells. C) Cell lysates from cultures treated for 24h with either DMSO (C), Das, PP2 or SU (as above) were probed for pY925-Fak, pY118-Paxillin, pY14-Caveolin-1; p130CAS was immunoprecipitated from total cell extracts and immuno-complexes analyzed by WB with anti-pY (4G10). Membranes were reblotted with anti-total-protein as loading control. Results are representative of three independent experiments. Ratios of phosphorylated/total-protein were normalized versus control cells. D) Cell migration by wound healing assay after treatment with DMSO, Dasatinib, PP2 or SU6656 (as above) for 20h. Fields are representative of three independent experiments performed in triplicates. Magnification, x100. E) For invasiveness, cells ($5x10^4$) were seeded on modified Boyden chamber coated with Matrigel in serum-free media containing DMSO (C), Das, PP2 or SU (as above). After 24h, cells on the lower surface of the filters were DAPI-stained and counted (see Materials and methods). Four independent experiments were made in triplicates. *$p<0.05$, **$p<0.01$ (Student *t*-test).

Fig. 2. Effects of Dasatinib, PP2 and SU6656 on MDA-MB-231 cell cycle progression, $p27^{Kip1}$ and c-Myc expression, morphological features. A) Cell cycle analysis by pulse/chase BrdU and PI labeling of cells treated with DMSO (Control), Dasatinib (100nM), PP2 (5μM) or SU6656 (5μM). Cells were collected at indicated times and analyzed by flow cytometry. Results are expressed as percentage of BrdU-labeled cells in the G1, S, and G2/M phases, as defined by PI label. Results represent the average±SD of four independent experiments. B) Cell cycle analysis by PI labeling of MDA-MB-231 after treatments with DMSO (C), Das, PP2, SU (as above) for 72h. Cell percentages in cell cycle phases (sub-G1, G1, S, G2/M, >4N) were calculated from DNA histograms by CellQuest software. C) Lysates from cells treated for 24h with DMSO (C), Das, PP2 or SU (as above) were analyzed by WB for $p27^{Kip1}$ and c-Myc. Membranes were reblotted either with anti-α-tubulin or β-actin for loading control. Results are representative of three independent experiments. D) Immunofluorescence of cultures treated with DMSO (Control), Dasatinib, PP2 and SU6656 (as above) for 24h. Cells were labeled for DNA (DAPI, blue) and for microtubules (anti-α-tubulin, green). Representative images captured with a Nikon Eclipse 90i fluorescence microscope. Bar=10μm. Arrows show a multinucleated cell.

Fig. 3. Effects of Dasatinib, PP2 and SU6656 in SYF fibroblasts. A) Cell cycle analyses of SYF cells treated with DMSO (C), Das (100nM), PP2 (5μM) and SU (5μM) for 24h. PI labeling was carried out as in Fig. 2B. B) Cultures treated as above were labeled with DAPI and with anti-α-tubulin and analyzed by immunofluorescence as in Fig. 2D. Arrows indicate a multinucleated cell. Bar=10μm.

Fig. 4. Comparative effects of SU6656 and ZM447439 in MDA-MB-231 cells. A) Cell cycle analyses by PI labeling of cultures treated with DMSO (C), SU (5μM) or ZM447439 (ZM, 5μM) for 24h were performed as in Fig. 2B. B) Immunofluorescence of cells labeled with DAPI and with anti-α-tubulin performed as in Fig. 2D. Arrows show multinucleated cells. Bar=10μm. C) Histone H3 phosphorylation (pS10-H3) determined by WB in extracts of cell treated with DMSO (C), SU or ZM (as above) for 24h. Membranes were blotted against anti-histone H3 (H3) for loading control. Results are representative of three independent experiments. D) Aurora B kinase was immunoprecipitated from cultures treated with DMSO (C) or SU (5μM) for 24h. Immune-complexes were incubated with histone H3 in the presence or absence of SU6656 (1μM) and ATP; the extent of S10-H3 phosphorylation determined by WB. Membranes were reblotted with anti-histone H3 and anti-Aurora B kinase for loading control. Results are representative of three independent experiments. E) Immunofluorescence micrographs of mitotic MDA-MB-231 cells. Control and treated cells (SU6656 or ZM447439 at 5μM, 24h) were labeled for DNA (DAPI, blue), microtubules (anti-α-tubulin, green) and pS10-histone H3 (anti-pS10-H3, red). Representative images of mitotic figures show multiple spindle poles in inhibitor-treated cells.

Fig. 5. Gene expression profiles regulated by Dasatinib, PP2 and SU6656. A) Hierarchical clustering (heat map) of all individual data representing the differentially expressed sequences after the three treatments at P*adjust* ≤0.05. Columns correspond to samples; row corresponds to individual probe sets. Intensities were normalized across the rows. Normalized log intensity values of probes were centered to the median value of each probe set and colored on a range of +2 (red) and -2 (blue); white indicates intermediate value. B) Comparisons between effects of Dasatinib, PP2 and SU6656 treatments are shown in plot profiles. Signal intensities are normalized as in the heat map and expression values are colored based on the overall pattern. For each pattern, a loess (locally weighted polynomial regression) fit line describes the overall profile of the corresponding group. This tendency profile is plotted up-regulated sequences (Cluster 1, green) and down-regulated sequences (Cluster 2, orange).

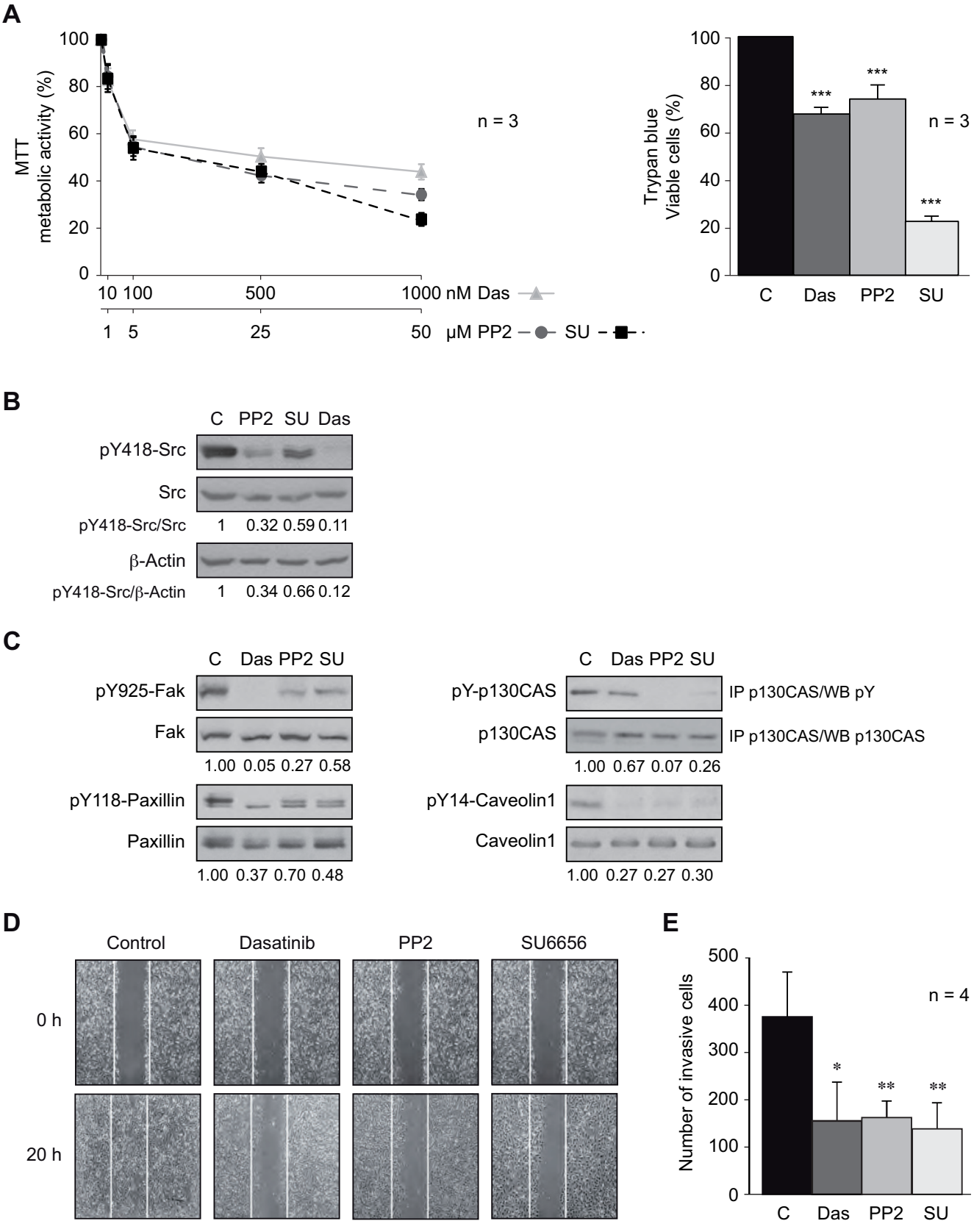
A
MTT metabolic activity (%)
100
80
60
40
20
0
10 100 500 1000 nM Das
1 5 25 50 μM PP2 SU
n = 3
Trypan blue Viable cells (%)
***
***
***
C Das PP2 SU
n = 3
B
C PP2 SU Das
pY418-Src
Src
pY418-Src/Src 1 0.32 0.59 0.11
β-Actin
pY418-Src/β-Actin 1 0.34 0.66 0.12
C
C Das PP2 SU
pY925-Fak
Fak
1.00 0.05 0.27 0.58
pY118-Paxillin
Paxillin
1.00 0.37 0.70 0.48
C Das PP2 SU
pY-p130CAS
p130CAS
IP p130CAS/WB pY
IP p130CAS/WB p130CAS
1.00 0.67 0.07 0.26
pY14-Caveolin1
Caveolin1
1.00 0.27 0.27 0.30
D
Control
Dasatinib
PP2
SU6656
0 h
20 h
E
Number of invasive cells
500
400
300
200
100
0
*
**
**
n = 4
C Das PP2 SU

Figure 1

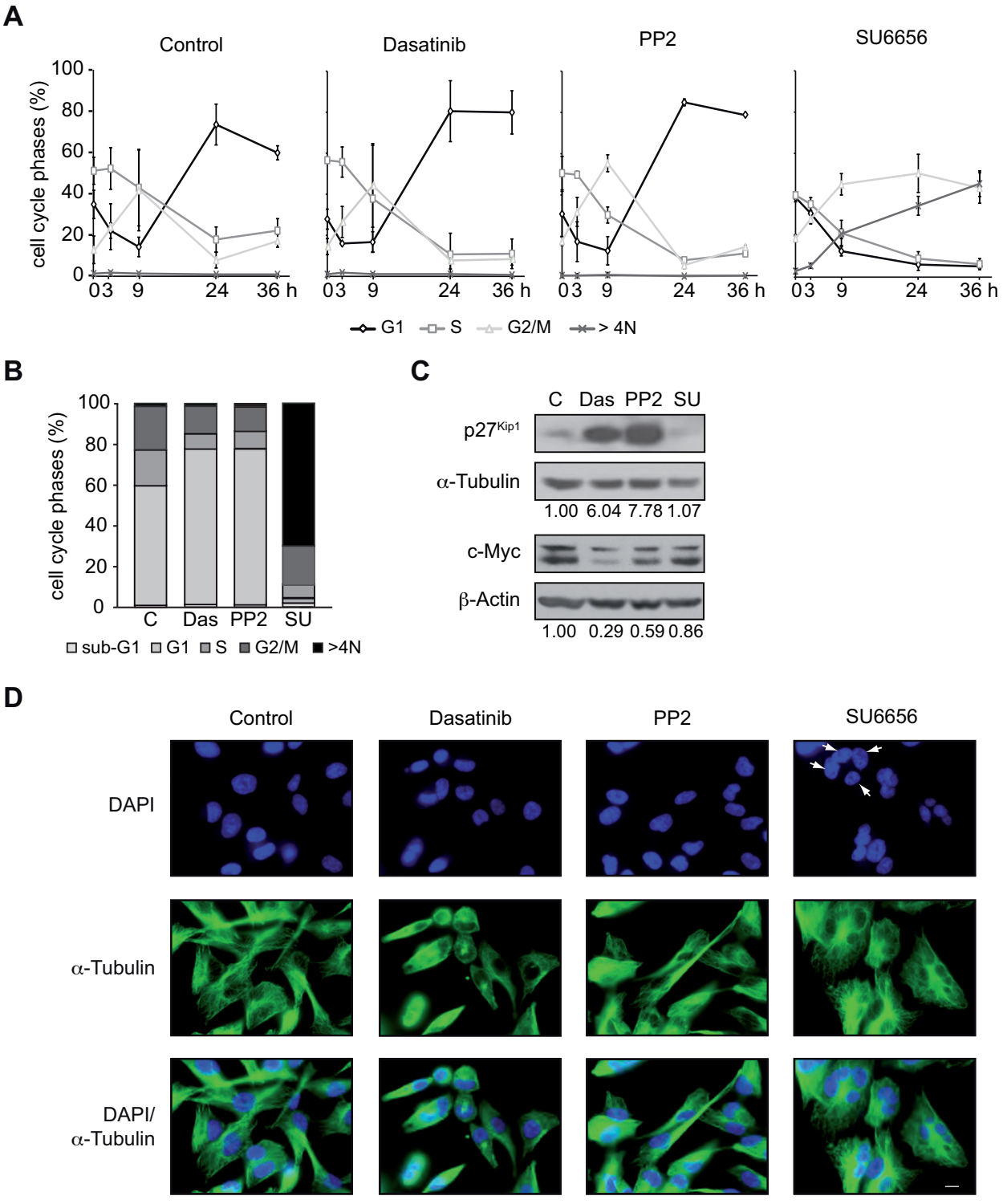
A
Control
Dasatinib
PP2
SU6656
cell cycle phases (%)
100
80
60
40
20
0
0 3 9 24 36 h
G1
S
G2/M
> 4N
B
cell cycle phases (%)
C
Das
PP2
SU
sub-G1
G1
S
G2/M
>4N
C
C Das PP2 SU
p27Kip1
α-Tubulin
1.00 6.04 7.78 1.07
c-Myc
β-Actin
1.00 0.29 0.59 0.86
D
Control
Dasatinib
PP2
SU6656
DAPI
α-Tubulin
DAPI/
α-Tubulin

Figure 2

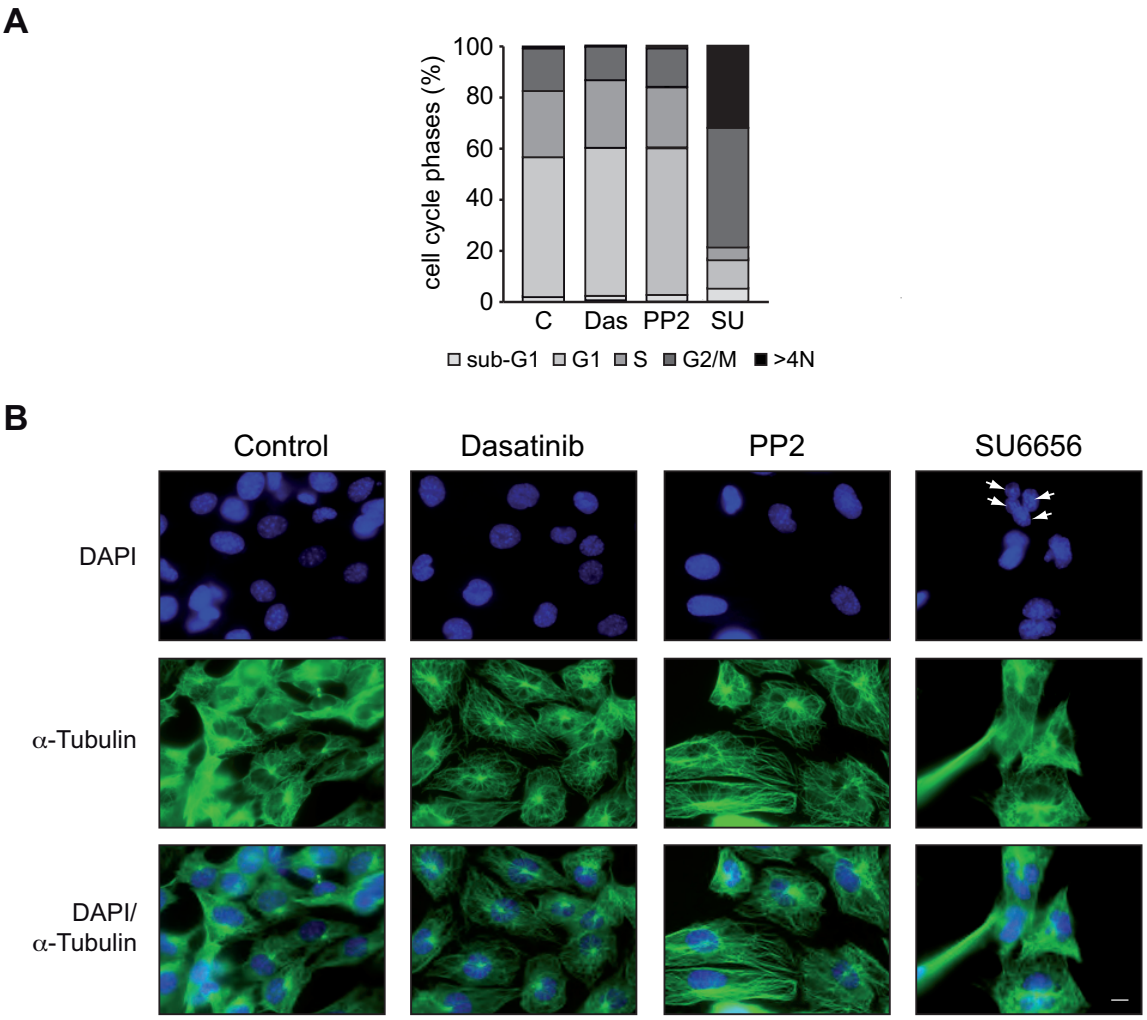
A
100
80
60
40
20
0
cell cycle phases (%)
C
Das
PP2
SU
sub-G1
G1
S
G2/M
>4N
B
Control
Dasatinib
PP2
SU6656
DAPI
α-Tubulin
DAPI/
α-Tubulin

Figure 3

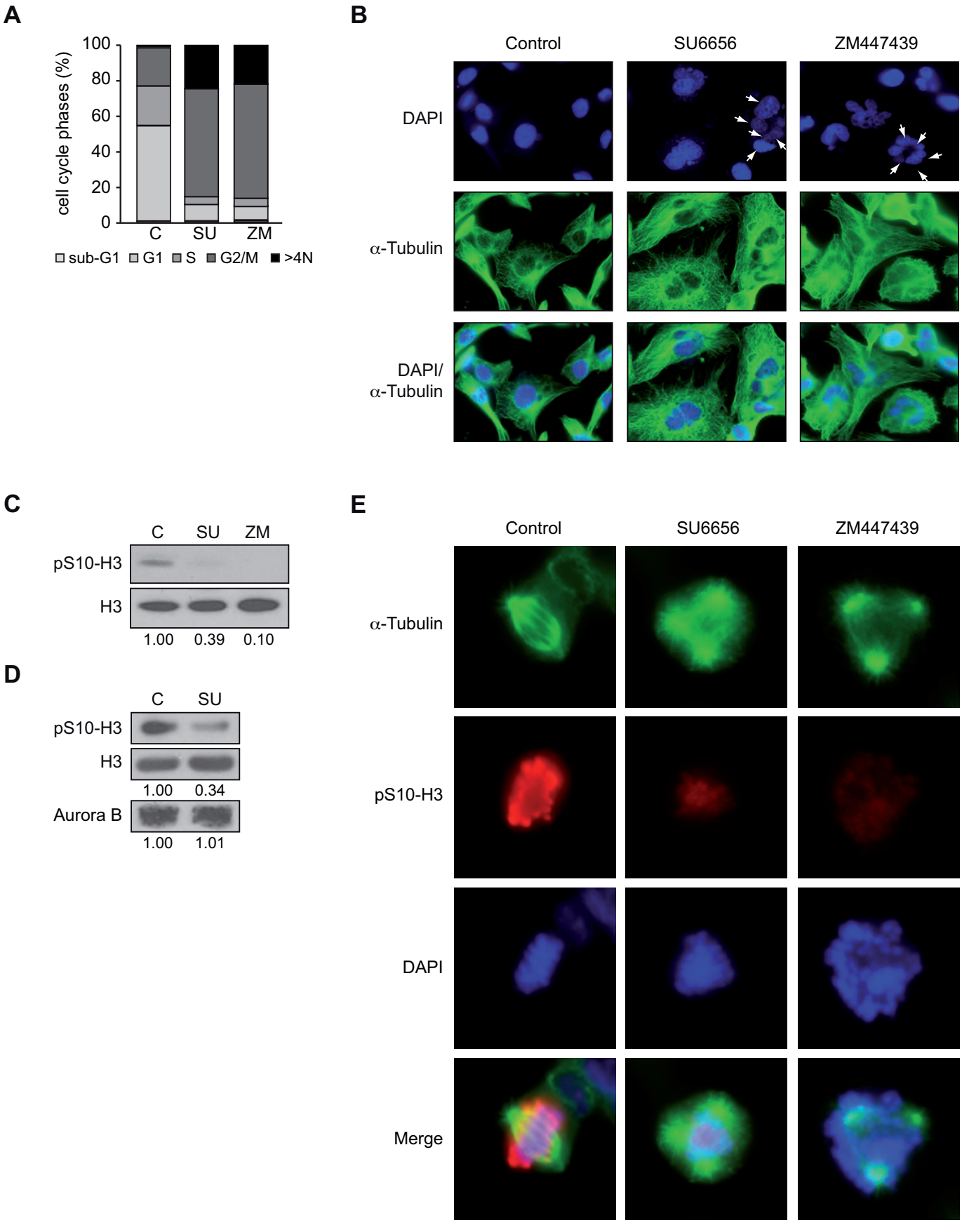
A
100
80
60
40
20
0
cell cycle phases (%)
C
SU
ZM
sub-G1
G1
S
G2/M
>4N
B
Control
SU6656
ZM447439
DAPI
α-Tubulin
DAPI/
α-Tubulin
C
C
SU
ZM
pS10-H3
H3
1.00
0.39
0.10
D
C
SU
pS10-H3
H3
1.00
0.34
Aurora B
1.00
1.01
E
Control
SU6656
ZM447439
α-Tubulin
pS10-H3
DAPI
Merge

Figure 4

A

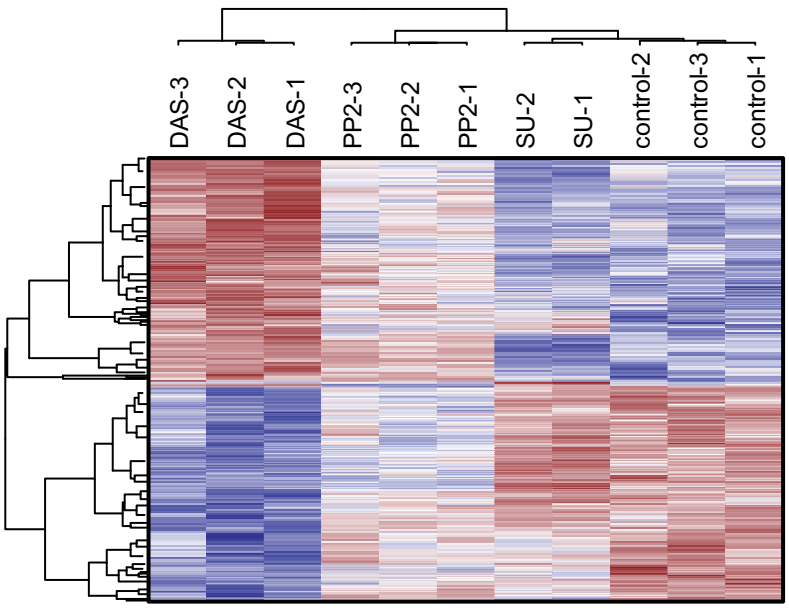
DAS-3
DAS-2
DAS-1
PP2-3
PP2-2
PP2-1
SU-2
SU-1
control-2
control-3
control-1

B

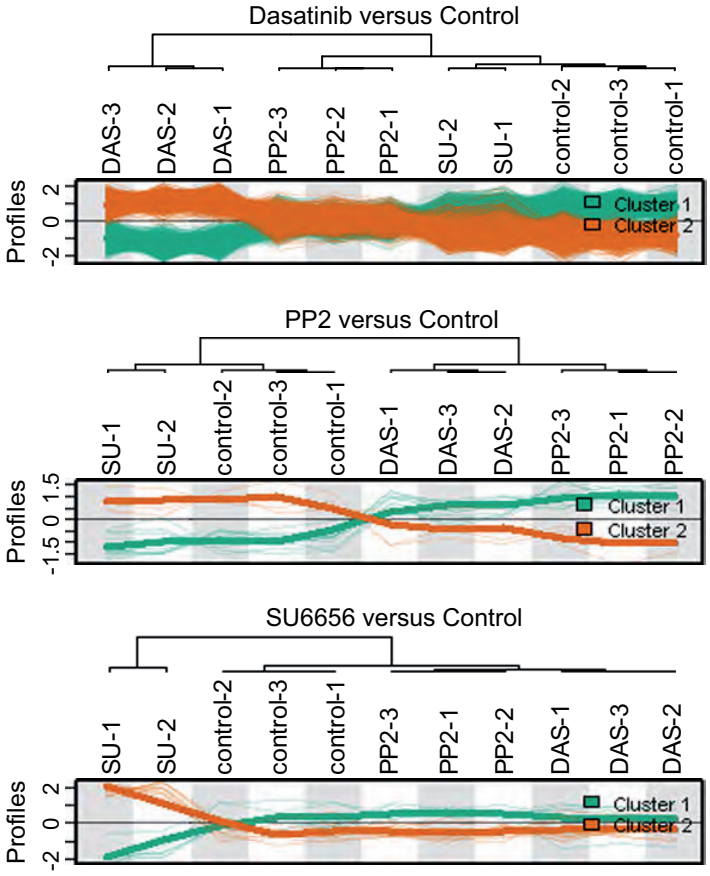
Dasatinib versus Control
DAS-3
DAS-2
DAS-1
PP2-3
PP2-2
PP2-1
SU-2
SU-1
control-2
control-3
control-1
Profiles
-2 0 2
Cluster 1
Cluster 2
PP2 versus Control
SU-1
SU-2
control-2
control-3
control-1
DAS-1
DAS-3
DAS-2
PP2-3
PP2-1
PP2-2
Profiles
-1.5 0 1.5
Cluster 1
Cluster 2
SU6656 versus Control
SU-1
SU-2
control-2
control-3
control-1
PP2-3
PP2-1
PP2-2
DAS-1
DAS-3
DAS-2
Profiles
-2 0 2
Cluster 1
Cluster 2

Figure 5